Revealing the relationship between molecular weight of lignin and its color, UV-protecting property

Yarong Li [a,b], Siyu Zhao [a,c], Yihan Li [a,b], Arthur J. Ragauskas [d,e,f], Xueping Song [a,c,*], Kai Li [a,b,*]

[a] College of Light Industry and Food Engineering, Guangxi University, Nanning 530004, P.R. China

[b] Engineering Research Center for Sugar Industry and Comprehensive Utilization, Ministry of Education, Nanning 530004, P.R. China

[c] Guangxi Key Laboratory of Clean Pulp & Papermaking and Pollution Control, Nanning, 530004, P.R. China

[d] Department of Chemical and Biomolecular Engineering, University of Tennessee, Knoxville, TN 37996, USA

[e] Joint Institute for Biological Sciences, Biosciences Division, Oak Ridge National Laboratory, Oak Ridge, TN 37771, USA

[f] Center for Renewable Carbon, Department of Forestry, Wildlife and Fisheries, The University of Tennessee, Knoxville, TN 37996, USA

*Corresponding author: sx_ping@gxu.edu.cn (Xueping Song), gxlikai@gxu.edu.cn (Kai Li)

Abstract: Lignin has great potential as a natural, green, and sustainable broad-spectrum sunscreen active ingredient. However, the coexistence of dark color and sunscreen properties hinders its application in cosmetics. In this study, we focus on the effects of the molecular weight of lignin on tis UV-protecting property and color in order to prepare lignin-based sunscreen with high performance. A prepared sunscreen containing low molecular weight lignin (F5, <1000 g/mol) exhibits good UV-protecting property (sun protection factor (SPF) = 7.14) and light color advantages (ΔE = 46.2). Moreover, a strong synergistic effect on UV-protecting property exists between low molecular weight lignin and ethylhexyl methoxycinnamate (EHMC), resulting in high SPF of F5@EHMC-based sunscreen (55.56). Additionally, added TiO_2 can efficiently mitigate the dark color of lignin-based sunscreens due to prominent covering power of TiO_2. Moreover, lignin-based sunscreens have good biocompatibility with HaCaT cells. This work is useful for understanding the mechanism of the UV-protecting property and dark color of lignin, and for designing an efficient and safe lignin-based sunscreen.

Keywords: Lignin, Molecular weight, Sunscreen, UV-protecting property, Color

1. Introduction

Lignin is a major component of plant cell walls and a biopolymer with natural reserves second to cellulose [1-3]. The global pulp and paper, and bioethanol refining industries produce nearly 70 million tons of lignin every year, but approximately 98 % of this is treated as low-value fuel or waste; essentially, the maximum value of lignin is not being used [4,5]. High-value utilization of lignin resources, by taking advantage of its unique properties, can effectively improve this situation. Notably, lignin has natural UV-protecting property; thus, the application of lignin as a green sunscreen active ingredient in cosmetics is promising and has attracted considerable attention in research [6-9]. At present, commercial sunscreen active ingredients primarily include chemical and physical ingredients, of which chemical ingredients account for 80 % [10]. Generally, chemical sunscreen active ingredients are small molecular aromatic compounds derived from unsustainable petrochemical resources, and their safety to humans is controversial [11-13]. In addition, chemical sunscreen active ingredients are increasingly polluting marine resources [14-17]. Thus, using lignin in sunscreen products not only produces natural, green, and safe sunscreen products but also reduces the pollution load of chemical sunscreens on marine resources.

Previous studies have reported that all types of lignin (such as alkali lignin, kraft lignin, and milled wood lignin) exhibit UV-protecting property [18]. Moreover, the conjugation system in lignin formed by its benzene ring and functional groups (such as carbonyl, carbon-carbon double bond, phenolic hydroxyl, and methoxy) can reduce the energy required for electronic transition; thus, lignin exhibits a broad absorption in the

58 UV spectrum range [6,19,20]. However, lignin has a dark color owing to the existence of
59 a conjugation system, and its dark color renders lignin-based sunscreen unpopular in
60 cosmetics [21]. Previously researchers in order to develop an excellent lignin dye
61 dispersant, have reported that lignin with high molecular weight (M_w = 18632, 14870
62 g/mol) has a darker color than lignin with a low molecular weight (M_w = 5143, 3746
63 g/mol) because high molecular weight lignin contains more conjugated carbonyl,
64 benzoquinone, and LCC structures [22,23]. Additionally, our previous work found that
65 phenolic hydroxyl and lignin-carbohydrate complex (LCC) structures in lignin are
66 important factors that simultaneously influence the UV protective performance and color
67 of lignin-based sunscreens [20,24]. Consequently, we think that the properties of lignin-
68 based sunscreen can been regulated by tailoring the molecular weight of lignin to obtain
69 a sunscreen with high performance. However, the relationships between the molecular
70 weight of lignin and its color, UV-protecting property, as well as the synergistic action of
71 lignin with different molecular weights and chemical and physical sunscreen active
72 ingredients on the UV-protecting property and color, have not been fully reported.
73 Therefore, a better understanding of these relationships is significant for the development
74 and application of lignin in cosmetics.

75 In this study, first, alkali lignin (AL) was fractionated with acetone/methanol as a co-
76 solvent and hexane as an anti-solvent, and five fractions of lignin with different molecular
77 weights were obtained. The physical and chemical structural differences of the lignin
78 samples were characterized by gel permeation chromatography (GPC), Fourier-transform
79 infrared (FTIR) spectroscopy, ^{31}P nuclear magnetic resonance (NMR), 2D-heteronuclear

single quantum coherence NMR (HSQC NMR), scanning electron microscopy (SEM), and contact angle tests to further analyze the effects of the chemical and physical differences of lignin samples on their UV-protecting property and color. Then, lignin-based sunscreens were prepared by mixing different lignin fractions with facial cream. The sun protection factor (SPF) and color difference (ΔE) of the lignin-based sunscreens were obtained to study the effect of the molecular weight of lignin on its UV-protecting property and color. Subsequently, the synergism of different lignin fractions and commercial chemical (ethylhexyl methoxycinnamate (EHMC)) and physical (TiO_2) active ingredients on UV-protecting property and color were explored. Finally, the lignin-based sunscreens' photostability and biocompatibility were evaluated. The obtained results promote the efficient utilization of lignin and offer a guidance for designing the high-performance lignin-based sunscreen.

2. Materials and methods

2.1. Materials

AL and 2-chloro-4,4,5,5-tetramethyl-1,3,2-dioxaphosporane (TMDP) were obtained from Sigma–Aldrich (St. Louis, MI). Impurities in AL are about 5% moisture, and AL is not purified before using. Analytically pure acetone, methanol, n-hexane, pyridine, acetic anhydride, anhydrous ethanol, deuterated chloroform, cyclohexanol, chromium acetylacetonate, deuterated dimethyl sulfoxide (DMSO), DMSO, 1,1-diphenyl-2-picrylhydrazyl (DPPH), EHMC, and TiO_2 were provided by Shanghai Macklin Biochemical Technology Co. Ltd. (Shanghai, China). HPLC-grade tetrahydrofuran (THF) was purchased from Tianjin Kemiou Chemical Reagent Co. Ltd. (Tianjin, China).

Polystyrene standards were purchased from Agilent Technologies Inc. (California, USA). Facial cream (Johnson) was purchased from a shopping mall.

2.2. Fractionation of AL

The fractionation process of AL was based on the method described by Wang, Li, Cai, Wyman and Ragauskas [25] and was adjusted appropriately. Briefly, 20 mg of AL were suspended in 200 mL of acetone/methanol (7:3, v/v) cosolvent and stirred at speed 600 rpm for 30 min at 25 °C. Subsequently, the mixture was centrifuged (8000 rpm, 4 °C), the precipitate and supernatant were collected, and the precipitate was labelled F1. The above steps were repeated, and 20, 40, and 60 mL of hexane were successively added to the supernatant to obtain different precipitates, which were labelled F2, F3, and F4, respectively. Next, the collected supernatant was concentrated at 40 °C, and a residue was obtained after the solvent was volatilized; this was labelled F5. The F1–F5 lignin fractions were vacuum-dried at 40 °C for 48 h to ensure that there was no solvent residue. Finally, the dried lignin samples were ground and sifted using a sieve (200-mesh) for experimentations.

2.3. Antioxidant activity of lignin samples

Lignin samples with different molecular weights were used to test the scavenging ability against DPPH free radicals to evaluate their antioxidant activity. DPPH was dissolved in ethanol to prepare a 0.1 mmol/L DPPH solution, and lignin was dissolved in DMSO to prepare lignin solutions at various concentrations. The resultant lignin solution (100 μL) was mixed with 2 mL DPPH solution, and the mixture was allowed to react for 60 min in the dark. The absorbance of the mixed solution was measured at 517 nm with

an Infinite M200 PRO microplate reader (TECAN, Austria). The DPPH inhibition percentage (IP) of lignin was calculated using Eq. (1):

$$DPPH\ IP\ (\%) = \frac{A_0 - (A_i - A_j)}{A_0} \times 100\% \quad (1)$$

, where A_0, A_i, and A_j are the absorbance values of DPPH blank solution, the mixed solution of lignin and DPPH, and the lignin solution, respectively.

2.4. Color measurement of samples

The color parameters of the samples (lignin and lignin-based sunscreen) were measured using a spectrophotometer (CS–420, CHN Spec, China), and the color difference between the sample and a reference whiteboard was calculated according to Eq. (2):

$$\Delta E = \sqrt{(\Delta L*)^2 + (\Delta a*)^2 + (\Delta b*)^2} \quad (2),$$

where $\Delta L*$, $\Delta a*$, and $\Delta b*$ are the color value differences between the sample and the white board.

2.5. Preparation of lignin-based sunscreens

By controlling the percentage of lignin, different lignin-based sunscreens were obtained by blending lignin samples (AL, F1–F5) with facial cream. For example, 1 wt.% AL-based sunscreen was prepared by magnetic stirring 4 mg of AL with 396 mg of facial cream at 1000 rpm for 3 h in the dark; 5 wt.% and 10 wt.% AL-based sunscreens were similarly obtained. Similarly, F1–F5 lignin-based sunscreens containing different lignin contents were prepared. Moreover, 10 wt.% lignin@EHMC-based sunscreen and 10 wt.% lignin@TiO_2-based sunscreen were prepared to explore the synergism of chemical and physical sunscreen active ingredients and lignin. For example, 10 wt.% AL@EHMC-

based sunscreen was prepared by blending 20 mg of AL and 20 mg of EHMC together with 360 mg of cream, and 10 wt.% AL@TiO_2-based sunscreen was prepared by blending 20 mg of AL and 20 mg of TiO_2 together with 360 mg of cream. Similarly, the 10 wt.% F1–F5 lignin@EHMC-based sunscreens and the 10 wt.% F1–F5 lignin@ TiO_2-based sunscreens were prepared.

2.6. Photostability of lignin-based sunscreen

Lignin-based sunscreens' photostability was characterized by an aging test. In particular, the surface of a quartz plate with an area of 16 cm^2 was adhered with 3M Transpore Tape, and 32 mg of the prepared sunscreen sample were evenly applied to the surface of the tape. Next, the quartz plate was placed under a UVA lamp tube (UVA 340, LONGPRO, China) and irradiated with UV light for 3 h. The distance between the lamp tube and quartz plate was approximately 5 cm.

2.7. Biocompatibility of lignin-based sunscreen

The sunscreen cytotoxicity of F5@C, F5@EHMC@C, and F5@TiO_2@C toward cultured human keratinocyte (HaCaT) cells was determined using the CCK8 method. The mass of the prepared sunscreens was 10 wt.%. First, the sunscreen sample was dispersed in Dulbecco's modified Eagle medium (DMEM) to obtain suspensions at concentrations of 0.2, 0.4, 0.8, 1, 2, 4, 8, and 10 mg/mL. Next, the prepared sunscreen suspensions were co-cultured with HaCaT cells for 24 h, and their absorbance values were measured at 450 nm using an EPOCH2 microplate reader (Biotek, USA). Calcein-AM and propidium iodide (PI) respectively stained the living and dead HaCaT cells, which was treated with sunscreens at concentration of 10 mg/mL, to observe the changes in cell morphology. The

168 relative viability of HaCaT cells was calculated using Eq. (3):

169 $Relative\ viability\ (\%) = \frac{A_{sample} - A_{blank}}{A_{control} - A_{blank}} \times 100\%$ (3), where

170 A_{sample} is the absorbance of a mixture containing DMEM, sunscreen sample, HaTaC cells,

171 and CCK8; $A_{control}$ is the absorbance of a mixture containing DMEM, HaTaC cells, and

172 CCK8; and A_{blank} is the absorbance of the mixture containing DMEM and CCK8.

173 **2.8. Characterization and calculation**

174 The molecular weights of the lignin samples were measured using a versatile GPC

175 analyzer (AGILENT 1260, Agilent, USA) equipped with a GPC column (PLgel MIXED-

176 E, 7.5 mm × 300 mm, 3 μm, Agilent, USA). An AVANCE III 500 Hz NMR instrument

177 (Bruker, Germany) was used to determine the ^{31}P NMR and 2D HSQC NMR spectra of

178 the lignin samples. The FTIR spectra of the lignin samples were obtained using a Thermo

179 Scientific Nicolet iS20 spectrometer (ThermoFisher Scientific, USA). The method used

180 for determining the bulk density of lignin was based on a previous study [26]. The water

181 contact angle of lignin was measured using a contact angle measuring instrument

182 (DSA100, KRUSS, Germany). Micrographs of the lignin samples were obtained by SEM

183 (TESCAN MIRA LMS, Czech), and the morphological characteristics of the lignin-based

184 sunscreen samples were observed using an optical microscope (Leica DM2500,

185 Germany). The UV transmittance measurement and SPF calculation of the sunscreens

186 were performed as described in our previous work [20].

187 **3. Results and discussion**

188 **3.1. Physical and chemical properties and antioxidant activity of lignin samples**

189 AL was fractionated using the solvent method to obtain five lignin samples with

different molecular weights, and the yields and molecular weight distributions of the obtained samples are listed in Table 1. The molecular weight of AL is 3313 g/mol and its polydispersity index (PDI) is 7.16, indicating that AL has a wide range of molecular weight distribution. F1 has the highest molecular weight of 9692 g/mol among the fractionated lignin samples, and its PDI is 3.64. The molecular weight and PDI of F2, F3, F4, and F5 decrease gradually, with F5 having the lowest molecular weight and PDI of 844 g/mol and 1.63, respectively. This suggests that lignin fractions with narrow molecular weight distribution are obtained by fractionation of AL.

Significant differences in the colors of AL and F1–F5 are observed in Table 1. The smaller the ΔE value, the closer the color of the lignin sample is to white [27]. From F1 to F4, the ΔE values gradually decrease, indicating that the colors of F1 to F4 gradually become lighter. However, F5 has the highest ΔE value (57.2) among the lignin samples; this indicates that F5 has the darkest color, which is consistent with the results observed by the naked eye (Fig. 1). Zhang, Chen, Liu and Fu [26] reported that the bulk density of lignin has a significant effect on its color. The higher the bulk density, the higher the chromophore concentration, which makes the lignin darker. Table 1 lists the bulk densities of the lignin samples. AL has the lowest bulk density (0.44 g/cm^3) among the lignin samples. Among the fractionated lignin samples, F1, F2, F3, and F5 have higher bulk densities of approximately 0.65 g/cm^3 compared with that of F4 (0.55 g/cm^3). SEM was used to observe the micro-morphology of the lignin samples (Fig. 1); evidently, AL is loosely stacked compared with F1–F5, which is consistent with the measured lowest bulk density of AL. The surfaces of the five lignin samples (F1–F5) obtained by

fractionation are relatively dense compared with that of AL, but the surface of F4 contains some large holes, which may be the reason for its lower bulk density compared with F1, F2, F3, and F5. Based on the above analysis, the ΔE values of F1–F4 are positively correlated with their bulk density. However, the color of AL and F5 does not depend only on their bulk density; this may be owing to their difference in chemical structure.

The chemical structure of the lignin samples was analyzed using FTIR, ^{31}P NMR, and 2D HSQC NMR. No additional absorption peak in the FTIR spectra of F1–F5 is observed compared with that of AL (Fig. 2(a)), which indicates that the fractionation method adopted in this study does not change the chemical structure of the lignin fractions. F5 has the strongest absorption peak at 1700 cm^{-1} in all samples because of the stretching vibration absorption generated by the conjugated carbonyl group [28]. Studies have reported that the conjugated system formed by carbonyl and benzene rings in lignin can reduce the energy required for the π→π* transition, thereby enhancing the light absorption capacity of lignin in the ultraviolet–visible (UV–Vis) region (290–800 nm) [6,29]; therefore, the dark color of F5 could be attributable to a high concentration of carbonyl groups. ^{31}P NMR characterization can be used to assign lignin's various hydroxyl groups (Fig. 2(b)), and the content of hydroxyl groups can be calculated through peak area integration [9]. The results are presented in Table 2. From F1 to F5, the content of aliphatic OH gradually decreases, whereas the content of phenolic OH gradually increases. The content of phenolic OH in F5 is 4.18 mmol/g, which is higher than that of the other lignin fractions. Phenolic OH is an important auxochrome group in lignin because it can form a p-π conjugated system with a benzene ring to enhance the light

234 absorption of lignin in the UV–Vis region [21]. Therefore, the presence of a high
235 concentration of phenolic OH groups in F5 is another important factor contributing to its
236 dark color. By assigning signals in the 2D HSQC NMR spectra of AL and F1–F5 (Fig.
237 2(c)), information on the connecting bonds and substructures in lignin can be obtained.
238 In region of δC/δH (50−90/2.5−6 ppm), the signals at δC/δH (59.1/3.60 ppm), δC/δH
239 (71.0/4.70 ppm), and δC/δH (84.5/4.23 ppm) are assigned to Cγ−Hγ, Cα−Hα, and Cβ−Hβ
240 in the β-O-4' substructure (A), respectively [30]. Compared with other samples, F5
241 contains the weakest signals for Cγ−Hγ and Cα−Hα; moreover, the Cβ−Hβ signal does
242 not appear in F5, which indicates that the content of β-O-4' substructure (A) in F5 is very
243 low. This further confirms that the phenolic hydroxyl content in F5 exists predominantly
244 in the free form rather than condensed form in the β-O-4' aryl ether bond. These results
245 are consistent with the ^{31}P NMR results, which indicates that F5 contains abundant
246 phenolic hydroxyl groups (Table 2). In the aromatic region (δC/δH (90−135/6−8 ppm)),
247 the signal at δC/δH (127.8/7.59 ppm) attributed to C_6–H_6 in the oxidized (Cα=O) guaiacyl
248 units (G') exists only in F5 [31]. Signals for C_2−H_2 (δC/δH (112.0/7.40 ppm)) and C_6−H_6
249 (δC/δH (120.1/7.20 ppm)) of ferulate (FA) appear in both AL and F5 [30], and the C_6−H_6
250 signal appears in F4, which indicates that ferulate (FA) in AL is retained in the fractions
251 with small molecular weights during fractionation. The signal at δC/δH (126.0/6.90 ppm)
252 belonging to Cβ−Hβ in the terminal group structure of hydroxycinnamaldehyde (F') is
253 additionally observed in AL and F5 [32]. Therefore, F5 and AL contain abundant
254 conjugated C=O groups. These chemical structural differences lead to their dark color;
255 besides, these differences are expected to have considerable impact on the UV-protecting

property of lignin-based sunscreens.

The antioxidant activity of lignin samples with different molecular weights was evaluated by measuring the DPPH radical scavenging capacity of lignin, and the DPPH scavenging capacity of vitamin E (V_E) was used as a control. Among all the lignin samples, AL has the best antioxidant activity, and its DPPH IP reaches approximately 80 % when its concentration is 0.4–1 mg/mL (Fig. 3). The antioxidant activity of the same lignin gradually increases with increasing concentration from 0.1 to 0.4 mg/mL. However, at high concentrations (>0.4 mg/mL), the DPPH IP of all lignin samples is similar, at approximately 75 %. Additionally, the antioxidant activity of all lignin samples with low concentration (0.1 mg/mL) is better than that of V_E.

3.2. UV-protecting property and color of lignin-based sunscreens

The UV-protecting property and color of lignin-based sunscreens are shown in Fig. 4. According to Fig. 4(a), the facial cream's SPF is 1.01, which indicates that the facial cream has almost no UV-protecting property. When lignin was blended with the facial cream, the facial cream's SPF increases, and the SPFs of lignin-based sunscreens increase with increasing lignin concentration (1 wt.%, 5 wt.%, 10 wt.%). In addition, from F1 to F5, the SPFs of the lignin-based sunscreens exhibits a gradual upward trend, and the 10 wt.% F5-based sunscreen has the highest SPF of 7.14. Based on the above analysis, the SPF of sunscreen prepared using low-molecular-weight lignin is high. This result is consistent with the change in phenolic hydroxyl content in lignin fractions listed in Table 2; essentially, a high phenolic hydroxyl content in low molecular weight lignin fractions results in excellent UV-protecting property of lignin-based sunscreens. In contrast, 10 wt.%

AL prepared sunscreen's SPF is 4.74, which is higher than that of the F1−F4-based sunscreens. AL has a lower phenolic hydroxyl content (1.79 mmol/g) than F2−F4 (1.82−2.89 mmol/g); however, it has a higher content of conjugated carbonyl groups than F2−F4, as determined by 2D HSQC NMR analysis, which indicates that the conjugated carbonyl group is another important contributor to excellent UV-protecting property. Furthermore, F5 has the highest SPF not only because of its high phenolic hydroxyl content, but also because of its high concentration of conjugated carbonyl groups.

The color of lignin-based sunscreens is shown in Fig. 4(a), wherein the F5-based sunscreen has the lightest color ($\Delta E = 46.2$). However, the F5 lignin sample has the darkest color among all the lignin samples in the dry state ($\Delta E = 57.2$). Facial cream contains primarily water (90 %) and esters, whereas lignin is an amphiphilic substance, whose existing state in facial cream is likely to be affected by its amphiphilicity (Qian et al., 2016). Therefore, we theorize that the dispersion state of F5 lignin sample in facial cream is different from that of other lignin samples, thus resulting in the F5-based sunscreen having the lightest color. The lignin-based sunscreens were observed at a 40× magnification using an optical microscope (Fig. S1). Pure facial cream is a uniform oil-in-water (W/O) lotion. When F1−F4 are added to the facial cream, the W/O state disappears, and lignin is dispersed in the facial cream with large and irregular particles. In F5-based sunscreen, lignin is surrounded by water, and the sunscreen exists in the same W/O state as the pure facial cream. In addition, W/O droplets and irregular lignin particles can be observed in the AL-based sunscreen. The water contact angles of the lignin samples (Fig. 4(b)) revealed that F5 has the highest water contact angle (52.6°), followed

by AL (51.2°). After 20 s, the contact angles of F5 and AL decrease slightly, which indicates that F5 and AL are strongly hydrophobic. In contrast, water is completely absorbed after contact with F1−F4 for 20 s, which indicates that F1−F4 has strong hydrophilicity. Therefore, in F5-based sunscreen, lignin exists in the form of W/O droplets owing to its strong hydrophobicity. Consequently, we believe that the reason for the color difference of lignin-based sunscreen is that F1−F4 have strong hydrophilicity and are easy to disperse in the cream, thus resulting in the cream being stained by lignin, and a dark color. In contrast, F5 is uniformly dispersed in the cream in the form of small droplets, and the cream is not easily stained by lignin. Moreover, this dispersion state reduces the aggregation between lignin molecules and macroscopically reduces the chromophore concentration; thus, the overall color of the F5-based sunscreen is light. As shown in Fig. 4(a), after 3 h of UV irradiation, ΔSPF and ΔE of 10 wt.% lignin-based sunscreens fluctuate from –0.11 to 0.83 and from–0.1 to 1.1, respectively; this indicates that UV irradiation negligibly affects their UV-protecting property and color, and these lignin-based sunscreens have good photostability.

3.3. Synergism of lignin and EHMC on UV-protecting property and color

Lignin fractions and the commercial sunscreen active ingredient EHMC were blended with facial cream to prepare different sunscreens to investigate the synergism of lignin fractions and EHMC on UV-protecting property. As shown in Fig. 5, the pure facial cream has almost no UV-protecting property owing to its UV transmittance is close to 100 %. The EHMC@C sunscreen prepared with 5 wt.% EHMC and 95 wt.% facial cream in the UVB region (290−320 nm) has the UV transmittance less than 5 %, whereas the

UV transmittance in the UVA region (320−400 nm) is close to 100 %, which indicates that EHMC has good UVB resistance capability, but has little UVA protection. The F5@C sunscreen prepared by mixing 5 wt.% F5 with 95 wt.% facial cream has weaker resistance to UVB than EHMC-based sunscreen, but its UV resistance in the UVA region is better, which indicates that lignin has the potential to be a broad-spectrum sunscreen active ingredient. When 5 wt.% F5 and 5 wt.% EHMC were mixed with 90 wt.% facial cream to prepare 10 wt.% F5@EHMC@C sunscreen, the UV protection efficiency of sunscreen in the entire UVB−UVA region is considerably improved. The SPFs of 10 wt.% lignin@EHMC@C sunscreens are shown in Fig. 5. Among them, the SPF of F1@EHMC@C sunscreen is 15.73, which is lower than the superposition (16.26) of the SPFs of 5 wt.% F1@C sunscreen (1.58) and 5 wt.% EHMC@C sunscreen (14.68); this indicates that no synergistic effect on UV-protecting property between F1 and EHMC. Similarly, the existence of a weak synergistic effect between F2 and EHMC is proven. The SPFs of the F3@EHMC@C, F4@EHMC@C, and F5@EHMC@C sunscreens gradually increase, among which the SPF of F5@EHMC@C sunscreen reaches a maximum of 55.56, which is nearly four times higher than that of the EHMC@C sunscreen (14.68). These results indicate that with a decrease in the molecular weight of lignin, the synergistic effect between lignin and EHMC on UV-protecting property becomes strong. The 10 wt.% lignin@EHMC@C sunscreens were observed with a microscope at 40× magnification (Fig. S1). The 10 wt.% EHMC@C sunscreen is an W/O lotion. When AL and F1−F4 were added to the facial cream together with EHMC, both W/O droplets and irregular lignin particles are observed in the sunscreen. However, in

the F5@EHMC-based sunscreen, only W/O droplets and no lignin particles are observed, which indicates that F5 and EHMC are both surrounded by water molecules. Generally, the synergistic effect produced by lignin and commercial sunscreen active ingredients on UV-protecting property is due to the π–π* stacking interaction of their benzene rings, which enlarges the conjugation system between them, thus enhancing the UV-protecting property of sunscreen [18]. The premise of the π–π* stacking interaction is that the two benzene rings are very close [33,34]. Therefore, in the F5@EHMC@C sunscreen, F5 and EHMC exhibit the strongest synergistic effect on the UV-protecting property among the fractionated lignin samples, thereby resulting in the highest SPF of the F5@EHMC@C sunscreen. After UV irradiation for 3 h, the SPFs of the lignin @EHMC@C sunscreens change slightly (Fig. 5), and their color does not change significantly (similar to Fig. 4(a)), which indicates that these lignin@EHMC@C sunscreens have good photostability.

3.4. Synergism of lignin and TiO_2 on UV-protecting property and color

TiO_2 is a commonly used inorganic sunscreen active ingredient and is a white pigment with strong covering power [35]. A 10 wt.% lignin@TiO_2@C sunscreen was prepared by blending 5 wt.% lignin and 5 wt.% TiO_2 with 90 wt.% facial cream to study the contribution of TiO_2 to the color reduction and UV-protecting property of lignin-based sunscreen. As shown in Fig. 6, the AL and F1–F4 lignin samples are evenly dispersed with TiO_2 in the facial cream. The ΔE values of AL and F1–F4@TiO_2@C sunscreens are approximately 40, which are lower than the ΔE values (approximately 50) of sunscreens prepared with AL and F1−F4@C; this indicates that TiO_2 can neutralize the dark color of lignin and effectively reduce the color of lignin-based sunscreens. The SPFs of AL and

F1−F4@TiO_2-based sunscreens are approximately equal to the added of SPFs of the lignin-based sunscreen and TiO_2-based sunscreen, which indicates that synergism between lignin and TiO_2 on the UV-protecting property does not exist. The sunscreen prepared with F5@TiO_2 has the lightest color ($\Delta E = 29.0$); however, F5 aggregates in the system (Fig. S1), which destroys its excellent sunscreen performance and leads to a SPF of only 3.73. Consequently, TiO_2 can efficiently improve the dark color of lignin-based sunscreen while contributing to the UV-protecting property of sunscreens prepared using lignin samples with molecular weights higher than 1000 g/mol. After UV irradiating for 3 h, the change ranges of SPFs and ΔE values of the prepared sunscreen samples are only -0.06−-0.64 and 1.1−1.6, respectively. Compared with the control group (TiO_2-based sunscreen), these changes are almost entirely caused by the light instability of TiO_2, which further indicates that lignin has good photostability.

3.5. Biocompatibility of lignin-based sunscreen

Biocompatibility and safety of lignin-based sunscreens are critical for their development. Based on the above analysis, F5 lignin has the most potential to be used in sunscreen; therefore, we selected F5@C, F5@EHMC@C, and F5@TiO_2@C sunscreens to test their cytotoxicity to HaCaT cells. The relative viabilities of HaCaT cells treated with different sunscreen samples are shown in Fig. 7. All of these sunscreens have little effect on the viability of HaCaT cells. Even at a high concentration treatment (10 mg/mL) of sunscreens, the relative viabilities reach more than 96 %. Moreover, the images of HaCaT cells treated with these sunscreens at a concentration of 10 mg/mL reveal that lignin-based sunscreens have almost no effect on the morphology of HaCaT cells.

Additionally, the relative viability of HaCaT cells after being treated with F5@C sunscreen is over 98.4 %, which is higher than that of F5@EHMC@C (96.5 %) and F5@TiO_2@C (96.4 %); this indicates that lignin has better biocompatibility and safety than commercial sunscreen active ingredients EHMC and TiO_2.

4. Conclusions

The effects of different molecular weights of lignin on color and UV-protecting property of lignin-based sunscreens were determined. The lower the molecular weight of lignin, the higher the SPF of the lignin-based sunscreen (F5@C sunscreen, SPF 7.14). At the same time, F5@C sunscreen has the lightest color because of its uniform W/O state. Moreover, the synergism of lignin samples and EHMC on the UV-protecting property is gradually enhanced with a decrease in the molecular weight of lignin (F5@EHMC@C sunscreen, SPF 55.56). Additionally, the dark color of lignin-based sunscreens can be efficiently improved by adding TiO_2. Moreover, lignin-based sunscreens exhibit excellent photostability and biocompatibility. This study offers a guidance for efficient utilization of lignin in the field of cosmetics. And combined with the recent advanced researches of lignin nanoparticle and decolorization of lignin by oxidant, it is very promising to overcome the obstacles of lignin application in cosmetics.

CRediT authorship contribution statement

Yarong Li: Data curation, Investigation, Writing–Original draft preparation. **Siyu Zhao:** Writing–review & editing. **Yihan Li:** Visualization, Investigation. **Arthur J. Ragauskas:** Writing–review & editing**. Xueping Song:** Supervision, Writing-Reviewing and Editing. **Kai Li:** Supervision, Funding acquisition.

Declaration of Competing Interest

The authors declare that they have no known competing financial interests or personal relationships that could have appeared to influence the work reported in this paper.

Acknowledgements

The project was sponsored by the National Key Research and Development Program of China (Grant No. 2021YFE0114400); the Natural Science Foundation of Guangxi Province, China (Grant No. 2021GXNSFDA196006); the Guangxi Innovation Driven Development Special Fund Project, China (Grant No. AA17204092); the National Natural Science Foundation of China (Grant No. 21766002); and the Foundation of Guangxi Key Laboratory of Clean Pulp & Papermaking and Pollution Control, College of Light Industry and Food Engineering, Guangxi University (grant nos. 2021KF02, 2021KF32, and 2021KF20). AJR efforts were funded by the University of Tennessee, Knoxville.

References

[1] X. Liu, F.P. Bouxin, J. Fan, V.L. Budarin, C. Hu, J.H. Clark, Recent advances in the catalytic depolymerization of lignin towards phenolic chemicals: A review, ChemSusChem 13(17) (2020) 4296-4317.

[2] P.P. Thoresen, L. Matsakas, U. Rova, P. Christakopoulos, Recent advances in organosolv fractionation: Towards biomass fractionation technology of the future, Bioresource Technol. 306 (2020) 123189.

[3] Z.-H. Liu, N. Hao, Y.-Y. Wang, C. Dou, F. Lin, R. Shen, R. Bura, D.B. Hodge, B.E.

Dale, A.J. Ragauskas, B. Yang, J.S. Yuan, Transforming biorefinery designs with 'plug-in processes of lignin' to enable economic waste valorization, Nat. Commun. 12(1) (2021) 3912.

[4] M. Gigli, C. Crestini, Fractionation of industrial lignins: Opportunities and challenges, Green Chem. 22(15) (2020) 4722-4746.

[5] J. Zhu, C. Yan, X. Zhang, C. Yang, M. Jiang, X. Zhang, A sustainable platform of lignin: From bioresources to materials and their applications in rechargeable batteries and supercapacitors, Prog. Energ. Combust. 76 (2020) 100788.

[6] Y. Zhang, M. Naebe, Lignin: A review on structure, properties, and applications as a light-colored UV absorber, ACS Sustain. Chem. Eng. 9(4) (2021) 1427-1442.

[7] L.A. Baker, B. Marchetti, T.N.V. Karsili, V.G. Stavros, M.N.R. Ashfold, Photoprotection: Extending lessons learned from studying natural sunscreens to the design of artificial sunscreen constituents, Chem. Soc. Rev. 46(12) (2017) 3770-3791.

[8] D. Piccinino, E. Capecchi, E. Tomaino, S. Gabellone, V. Gigli, D. Avitabile, R. Saladino, Nano-structured lignin as green antioxidant and UV shielding ingredient for sunscreen applications, Antioxidants 10(2) (2021) 274.

[9] Y. Qian, X. Zhong, Y. Li, X. Qiu, Fabrication of uniform lignin colloidal spheres for developing natural broad-spectrum sunscreens with high sun protection factor, Ind. Crop. Prod. 101 (2017) 54-60.

[10] M.H. Tran, D.-P. Phan, E.Y. Lee, Review on lignin modifications toward natural UV protection ingredient for lignin-based sunscreens, Green Chem. 23(13) (2021)

4633-4646.

[11] Y. Song, S. Liu, X. Jiang, Q. Ren, H. Deng, Y.N. Paudel, B. Wang, K. Liu, M. Jin, Benzoresorcinol induces developmental neurotoxicity and injures exploratory, learning and memorizing abilities in zebrafish, Science of the Total Environment 834 (2022) 155268.

[12] R.C. Romanhole, A.L.M. Fava, L.L. Tundisi, L.M.d. Macedo, E.M.d. Santos, J.A. Ataide, P.G. Mazzola, Unplanned absorption of sunscreen ingredients: Impact of formulation and evaluation methods, Int. J. Pharmaceut. 591 (2020) 120013.

[13] B. Du, Y. He, B. Liang, J. Li, D. Luo, H. Chen, L.-Y. Liu, Y. Guo, L. Zeng, Identification of triazine UV filters as an emerging class of abundant, ubiquitous pollutants in indoor dust and air from south china: Call for more concerns on their occurrence and human exposure, Environ. Sci. Technol. 56(7) (2022) 4210-4220.

[14] h. He, a. Li, s. Li, j. Tang, l. Li, l. Xiong, Natural components in sunscreens: Topical formulations with sun protection factor (SPF), Biomed. Pharmacother. 134 (2021) 111161.

[15] A. Jesus, E. Sousa, M.T. Cruz, H. Cidade, J.M.S. Lobo, I.F. Almeida, UV filters: Challenges and prospects, Pharmaceuticals 15(3) (2022) 263.

[16] M.M.P. Tsui, J.C.W. Lam, T.Y. Ng, P.O. Ang, M.B. Murphy, P.K.S. Lam, Occurrence, distribution, and fate of organic UV filters in coral communities, Environ. Sci. Technol. 51(8) (2017) 4182-4190.

[17] D. Stien, F. Clergeaud, A.M.S. Rodrigues, K. Lebaron, R.m. Pillot, P. Romans, S. Fagervold, P. Lebaron, Metabolomics reveal that octocrylene accumulates in

476 pocillopora damicornis tissues as fatty acid conjugates and triggers coral cell
477 mitochondrial dysfunction, Anal. Chem. 91(1) (2019) 990-995.
478 [18] Y. Qian, X. Qiu, S. Zhu, Sunscreen performance of lignin from different technical
479 resources and their general synergistic effect with synthetic sunscreens, ACS
480 Sustain. Chem. Eng. 4(7) (2016) 4029-4035.
481 [19] Y. Qian, X. Qiu, S. Zhu, Lignin: A nature-inspired sun blocker for broad-spectrum
482 sunscreens, Green Chem. 17(1) (2015) 320-324.
483 [20] Y. Li, S. Zhao, X. Song, D. Cao, K. Li, M. Hassanpour, Z. Zhang, UV-shielding
484 performance and color of lignin and its application to sunscreen, Macromol. Mater.
485 Eng. 307(2) (2022) 2100628.
486 [21] J. Wang, Y. Deng, Y. Qian, X. Qiu, Y. Ren, D. Yang, Reduction of lignin color via
487 one-step UV irradiation, Green Chem. 18(3) (2016) 695-699.
488 [22] H. Zhang, Y. Bai, B. Yu, X. Liu, F. Chen, A practicable process for lignin color
489 reduction: Fractionation of lignin using methanol/water as a solvent, Green Chem.
490 19(21) (2017) 5152-5162.
491 [23] H. Zhang, S. Fu, Y. Chen, Basic understanding of the color distinction of lignin and
492 the proper selection of lignin in color-depended utilizations, Int. J. Biol. Macromol.
493 147 (2020) 607-615.
494 [24] Y. Li, S. Zhao, D. Hu, A.J. Ragauskas, D. Cao, W. Liu, C. Si, T. Xu, P. Zhao, X.
495 Song, K. Li, Role evaluation of active groups in lignin on UV-shielding
496 performance, ACS Sustain. Chem. Eng. 10 (2022) 11856-11866.
497 [25] Y.-Y. Wang, M. Li, C. Cai, C. Wyman, A.J. Ragauskas, Fast fractionation of

technical lignins by organic cosolvents, ACS Sustain. Chem. Eng. 6(5) (2018) 6064-6072.

[26] H. Zhang, F. Chen, X. Liu, S. Fu, Micromorphology influence on the color performance of lignin and its application in guiding the preparation of light-colored lignin sunscreen, ACS Sustain. Chem. Eng. 6(9) (2018) 12532-12540.

[27] S.C. Lee, T.M.T. Tran, J.W. Choi, K. Won, Lignin for white natural sunscreens, Int. J. Biol. Macromol. 122 (2019) 549-554.

[28] A. Tejado, C. Pen˜a, J. Labidi, J.M. Echeverria, I. Mondragon, Physico-chemical characterization of lignins from different sources for use in phenol-formaldehyde resin synthesis, Bioresource Technol. 98(8) (2007) 1655-1663.

[29] A.C.P.d. Silvaa, J.P. Paivab, R.R. Diniz, V.M.d. Anjos, A.B.S.M. Silva, A.V. Pinto, E.P.d. Santos, A.C. Leitão, L.M. Cabral, C.R. Rodrigues, M.d. Pádula, B.A.M.C. Santos, Photoprotection assessment of olive (olea europaea l.) leaves extract standardized to oleuropein: In vitro and in silico approach for improved sunscreens, J. Photoch. Photobio. B. 193 (2019) 162-171.

[30] H.-Y. Li, B. Wang, J.-L. Wen, X.-F. Cao, S.-N. Sun, R.-C. Sun, Availability of four energy crops assessing by the enzymatic hydrolysis and structural features of lignin before and after hydrothermal treatment, Energ. Convers. Manage. 155 (2018) 58-67.

[31] J.-L. Wen, B.-L. Xue, F. Xu, R.-C. Sun, A. Pinkert, Unmasking the structural features and property of lignin from bamboo, Ind. Crop. Prod. 42 (2013) 332-343.

[32] J.-L. Wen, S.-L. Sun, B.-L. Xue, R.-C. Sun, Quantitative structural characterization

of the lignins from the stem and pith of bamboo (phyllostachys pubescens), Holzforschung 67(6) (2013) 613-627.

[33] R. Thakuria, N.K. Nath, B.K. Saha, The nature and applications of π–π interactions: A perspective, Cryst. Growth Des. 19(2) (2019) 523-528.

[34] J.M. Živković, I.M. Stanković, D.B. Ninković, S.a.D. Zarić, Phenol and toluene stacking interactions, including interactions at large horizontal displacements. Study of crystal structures and calculation of potential energy surfaces, Cryst. Growth Des. 20(2) (2020) 1025-1034.

[35] K. Chen, X. Zhou, D. Wang, J. Li, D. Qi, Synthesis and characterization of a broad-spectrum tio2@lignin UV-protection agent with high antioxidant and emulsifying activity, Int. J. Biol. Macromol. 218 (2022) 33-43.

533 **Table 1** The physical properties of lignin samples.

Samples	Yields (%)	Molecular weight distributions			Color values				Color [a]	Bulk density (g/cm^3)
		Mw (g/mol)	Mn (g/mol)	PDI	L*	a*	b*	ΔE		
AL	—	3313	463	7.16	44.63	7.72	1.38	54.7	▲▲▲	0.44
F1	32.75	9692	2663	3.64	44.24	5.10	10.11	55.5	▲▲▲▲▲	0.67
F2	16.10	5992	2634	2.27	45.25	6.80	10.97	54.8	▲▲▲▲	0.65
F3	17.80	3351	1863	1.80	46.66	6.83	11.77	53.6	▲▲	0.64
F4	9.35	1975	1196	1.65	47.85	8.29	14.22	53.2	▲	0.55
F5	23.45	844	487	1.63	43.76	10.36	13.02	57.2	▲▲▲▲▲▲	0.62

534 [a] ▲ means the degree of color darkening.

535
536

537 **Table 2** Contents of hydroxyl groups in lignin samples.

Assignments	δ ppm	AL	F1	F2	F3	F4	F5
		mmol/g					
Aliphatic OH	148.91-144.97	2.16	2.99	2.51	2.33	2.05	1.42
C_5-substituted phenolic OH	143.99-141.17	0.21	0.32	0.16	0.37	0.79	0.78
Guaiacyl phenolic OH	141.14-137.98	1.48	1.09	1.61	2.31	1.95	3.15
p-Hydroxylphenyl phenolic OH	137.88-136.79	0.10	0.04	0.05	0.15	0.15	0.25
Carboxylic acid OH	135.29-133.04	0.25	0.22	0.29	0.27	0.21	0.37
Total OH		4.20	4.66	4.62	5.43	5.15	5.97
Total phenolic OH		1.79	1.45	1.82	2.83	2.89	4.18

538

539

540

Figure Captions

Fig. 1. Photographs and images of SEM (11.0 k×) of lignin samples.

Fig. 2. (a) FTIR spectra of AL and F1−F5. (b) ^{31}P NMR spectrum of F5 as an example. (c) 2D HSQC NMR spectra of AL and F1−F5 samples and main substructures identified in lignin samples, and the attribution of all signals can be found in Table S1.

Fig. 3. The DPPH inhibition percentage (IP) of lignin samples' solution at different concentrations, and V_E solution at different concentrations as control.

Fig. 4. UV-protecting property and color of lignin-based sunscreens: (a) photographs of 10 wt.% lignin-based sunscreens and SPF of lignin-based sunscreens with different concentrations, (b) water contact angle of lignin samples.

Fig. 5. SPFs of 10 wt.% sunscreens prepared by 5 wt.% lignin samples and 5 wt.% EHMC before and after 3 h UV irradiation, and 5 wt.% lignin-based sunscreens and 5 wt.% EHMC-based sunscreen are as control. The embedded diagram is UV transmittance spectra of sunscreens prepared by EHMC, F5, and F5@EHMC as examples.

Fig. 6. SPFs and ΔE values of 10 wt.% sunscreens (prepared by blending 5 wt.% lignin samples and 5 wt.% TiO_2 with facial cream) before and after 3 h UV irradiation, and 5 wt.% lignin-based sunscreens and 5 wt.% TiO_2-based sunscreen as control.

Fig. 7. (a) Viabilities of HaCaT cells treated with F5@C, F5@EHMC@C, and F5@TiO_2@C sunscreens, and (b) the images of HaCaT cells treated with these sunscreens at concentration of 10 mg/mL.

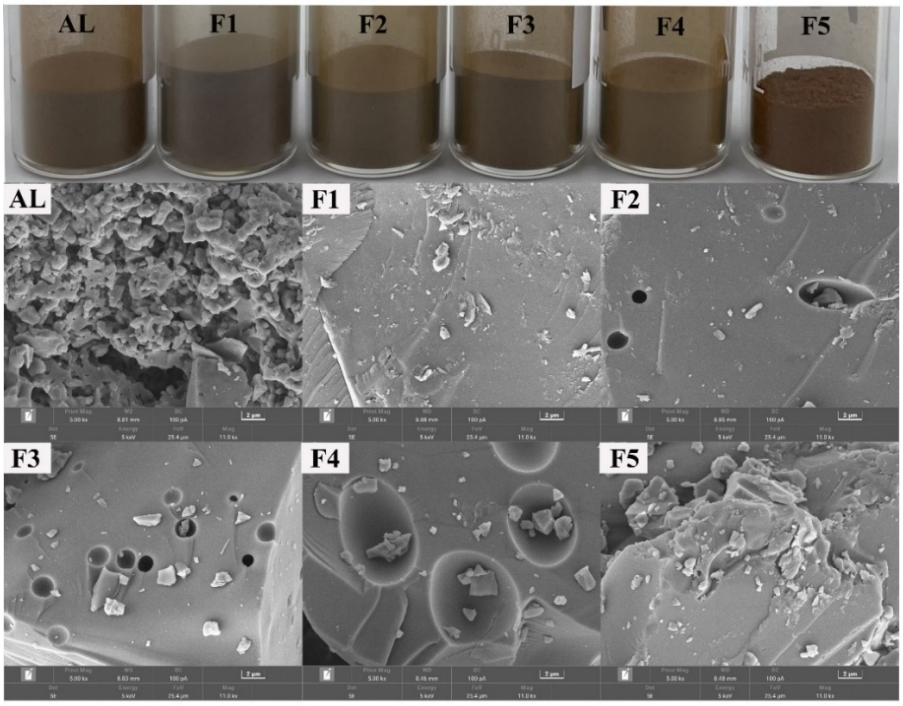

563

564 **Fig. 1.**

565

566

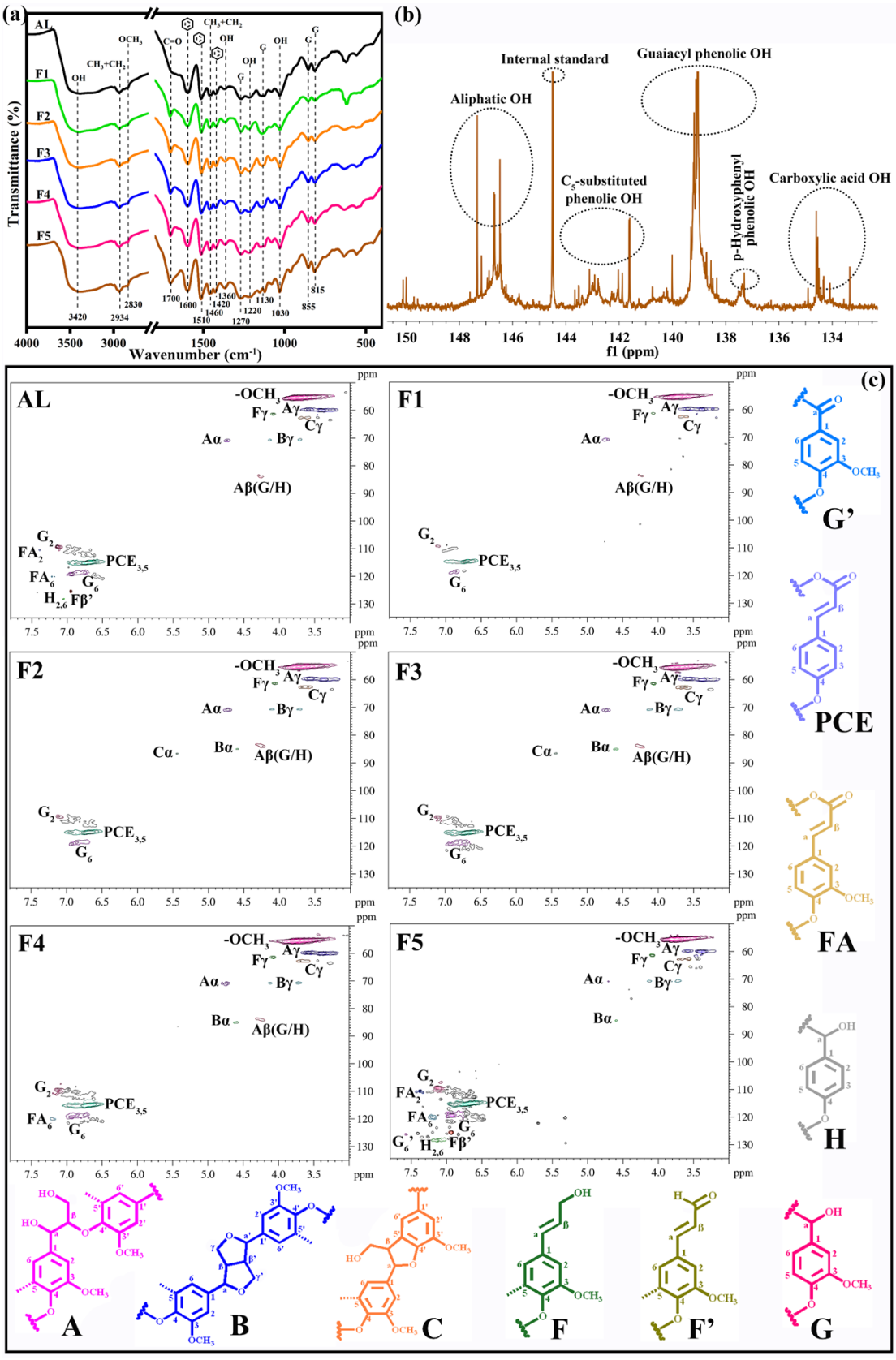
(a)
AL
F1
F2
F3
F4
F5
Transmittance (%)
Wavenumber (cm-1)
(b)
Internal standard
Guaiacyl phenolic OH
Aliphatic OH
C5-substituted phenolic OH
p-Hydroxyphenyl phenolic OH
Carboxylic acid OH
f1 (ppm)
(c)
AL
F1
F2
F3
F4
F5
-OCH3
Aγ
Fγ
Cγ
Aα
Bγ
Aβ(G/H)
Cα
Bα
G2
FA2'
PCE3,5
FA6'
G6
H2,6
Fβ'
G'
PCE
FA
H
A
B
C
F
F'
G

Fig. 2.

569

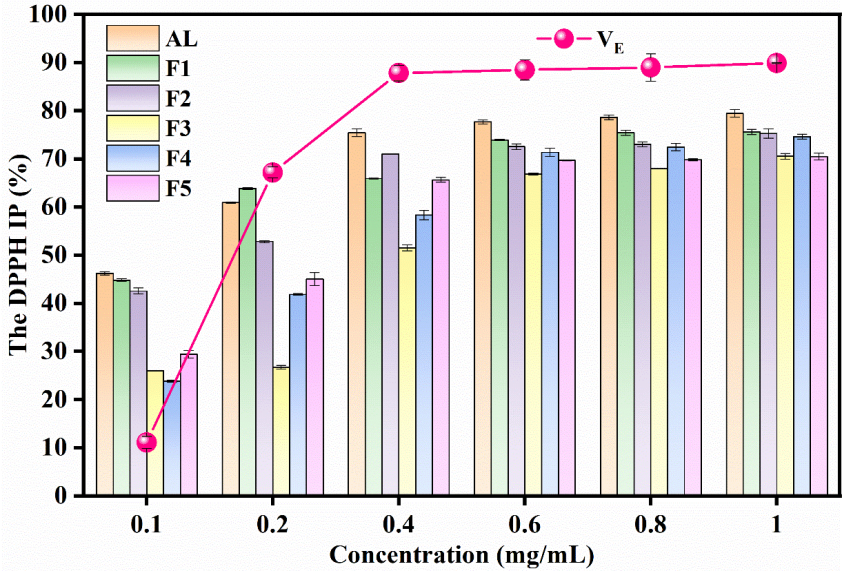

570

571 **Fig. 3.**

572

573

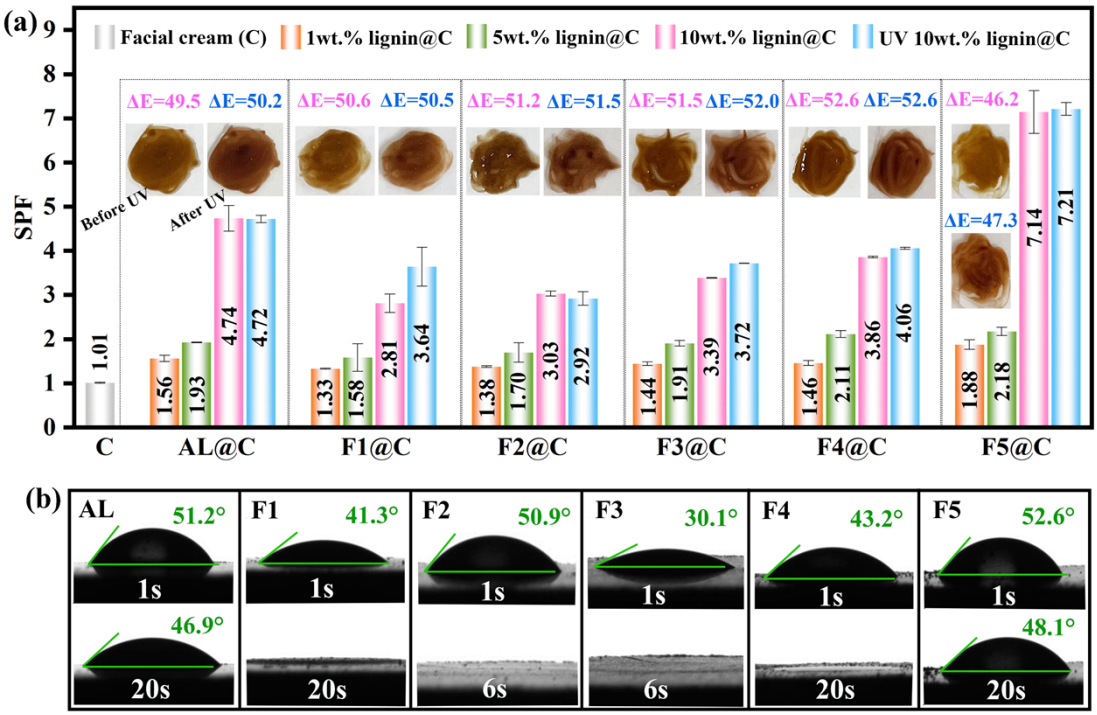

574

575 **Fig. 4.**

576

577

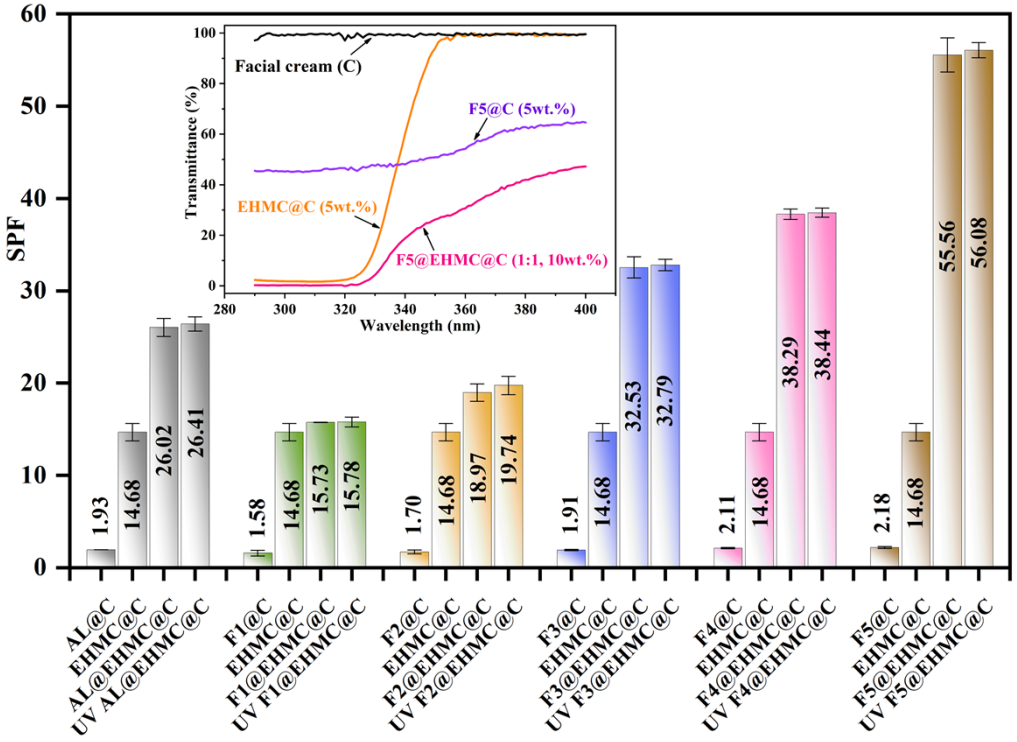
SPF
Transmittance (%)
Wavelength (nm)
Facial cream (C)
F5@C (5wt.%)
EHMC@C (5wt.%)
F5@EHMC@C (1:1, 10wt.%)
1.93
14.68
26.02
26.41
1.58
14.68
15.73
15.78
1.70
14.68
18.97
19.74
1.91
14.68
32.53
32.79
2.11
14.68
38.29
38.44
2.18
14.68
55.56
56.08
AL@C
EHMC@C
AL@EHMC@C
UV AL@EHMC@C
F1@C
EHMC@C
F1@EHMC@C
UV F1@EHMC@C
F2@C
EHMC@C
F2@EHMC@C
UV F2@EHMC@C
F3@C
EHMC@C
F3@EHMC@C
UV F3@EHMC@C
F4@C
EHMC@C
F4@EHMC@C
UV F4@EHMC@C
F5@C
EHMC@C
F5@EHMC@C
UV F5@EHMC@C

Fig. 5.

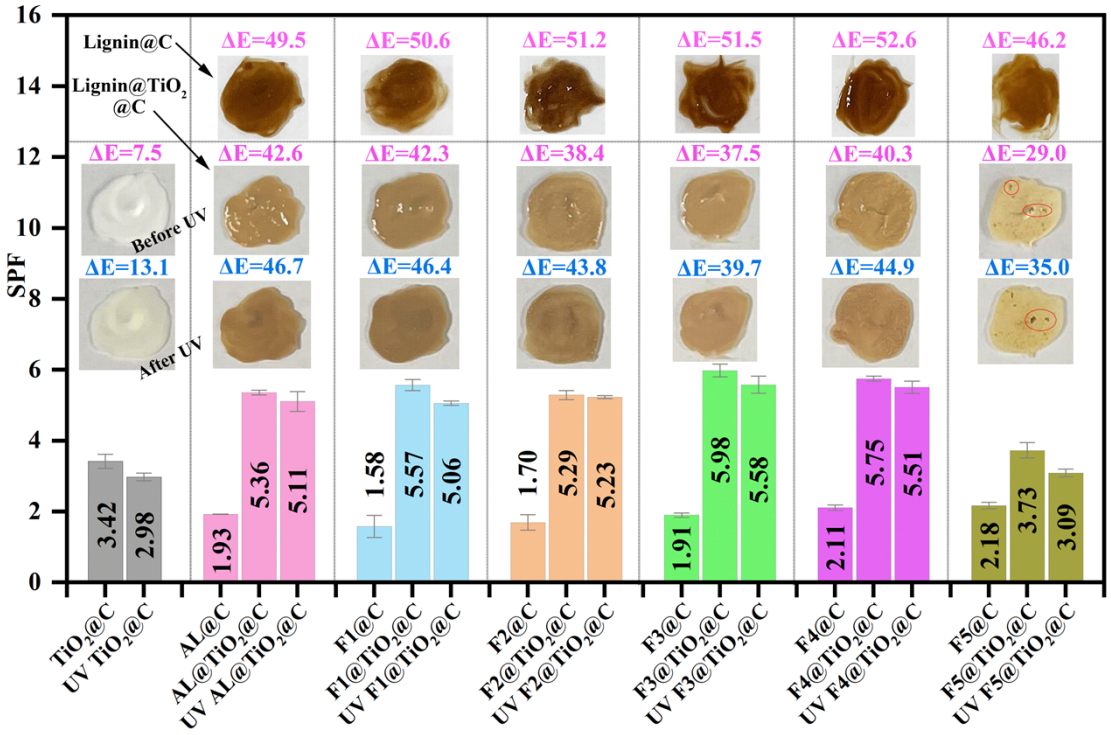

582

583 **Fig. 6.**

584

585

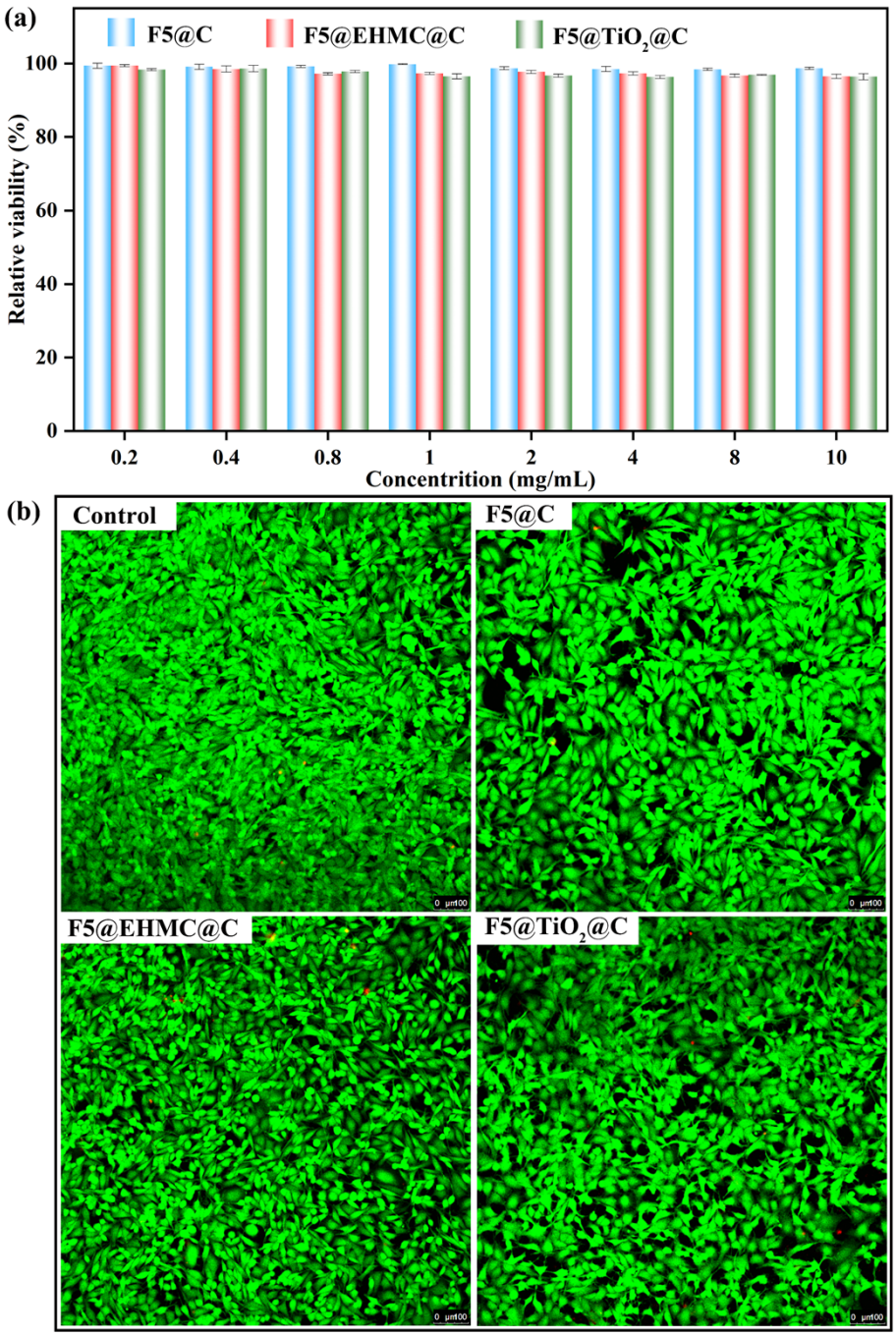

586

587 **Fig. 7.**

588

589

590 **Graphical Abstract**

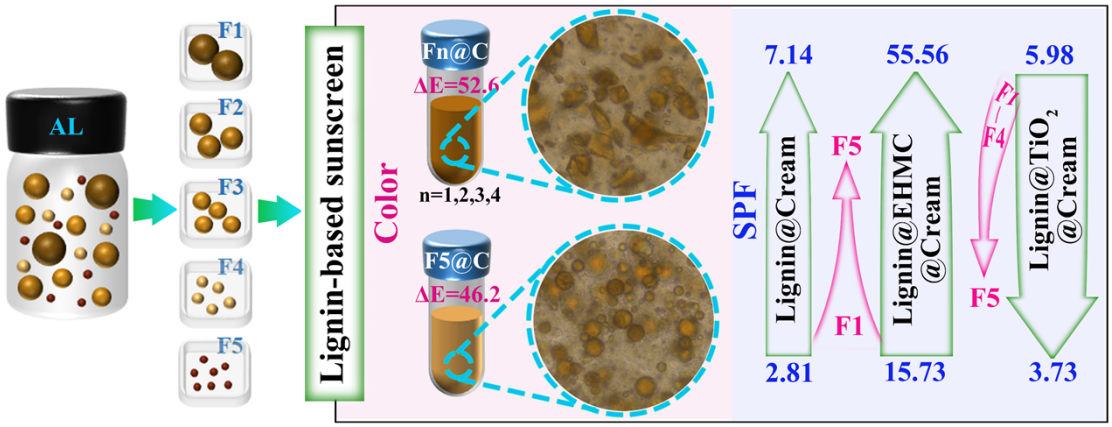

591

592